

Kinetic and Electronic Energy Dependence of the Reaction of  $V^+$  with  $D_2O$ D. E. Clemmer,<sup>†</sup> Yu-Min Chen, N. Aristov,<sup>‡</sup> and P. B. Armentrout\*

Department of Chemistry, University of Utah, Salt Lake City, Utah 84112

Received: March 9, 1994; In Final Form: May 20, 1994\*

The reaction of  $V^+$  with  $D_2O$  is studied as a function of translational energy in a guided-ion-beam tandem mass spectrometer. Three ionic products are formed:  $VD^+$ ,  $VO^+$ , and  $VOD^+$ . The effect of electronic energy is probed by varying the conditions used for forming  $V^+$ . The  $a^3F$  state of  $V^+$  reacts much more efficiently than the  $a^5D$  ground state in forming all three product ions. Indeed, excited triplet states of  $V^+$  dehydrogenate  $D_2O$  to form  $VO^+ + D_2$  very efficiently, while this reaction is not observed for  $V^+(a^5D)$  even though the reaction is exothermic. These results are consistent with a recent study of the reverse reaction of  $VO^+ + D_2$  [*J. Phys. Chem.* 1993, 97, 544]. State-specific cross sections suggest that the reaction occurs primarily through a triplet state  $D-V^+-OD$  intermediate and can be explained by using molecular-orbital and spin-conservation concepts. The threshold for endothermic formation of  $VOD^+$  is interpreted to give  $D_0(V^+-OD) = 4.41 \pm 0.19$  eV.

## Introduction

A long-term goal in our laboratories has been to characterize the activation of small molecules by atomic transition metal ions. State-specific studies of the periodic trends in this chemistry have provided insight into the electronic requirements for metal activation of  $H-H$ ,  $C-H$ ,  $C-C$ ,  $C-X$  (where  $X$  is a halogen atom), and  $N-H$  bonds.<sup>1</sup> Here, we extend this work to examine the activation of the  $O-D$  bonds of deuterated water. The interaction of transition metal centers with water is important for understanding catalytic processes such as those in Fischer-Tropsch and water gas-shift chemistry. The present study is also of interest because we have previously studied the interactions of  $V^+$  with ammonia<sup>2</sup> and methane,<sup>3</sup> molecules that are isoelectronic with water (in the sense that the central heavy atom has the same number of valence electrons with the same  $sp^3$  hybridization<sup>4</sup>).

In this work, guided-ion-beam mass spectrometry is used to study the reactions of  $V^+$  with  $D_2O$  as a function of relative collision energy. Through changes in the source conditions for producing the vanadium ions, the populations of excited state ions in the beam are systematically varied, thereby probing the effect of electronic excitation on the reaction. Results for this reaction system have not been described in detail in the literature previously, although Marinelli and Squires have noted that  $V^+$  in uncharacterized electronic states reacts to dehydrogenate  $H_2O$ .<sup>5</sup> A related result is our recent study of the collisional energy dependence for the reaction of ground state vanadium oxide ions with  $D_2$  to produce water (reaction 1).<sup>6</sup> Our results showed that



the threshold for this reaction is about 0.3 eV above the thermodynamic threshold for formation of ground state  $V^+(a^5D)$ . We found that this delayed reaction threshold could be modeled if we assumed that the ionic products were  $V^+(a^3F)$  and primarily  $V^+(a^3F)$ , the first and second excited states of  $V^+$ . The preference for formation of the  $a^3F$  state was rationalized by noting that this product channel is the lowest energy pathway that conserves spin in the reaction of ground state  $VO^+(^3\Sigma^-)$  and  $D_2(^1\Sigma_g^+)$ . An alternate interpretation of the delayed threshold for reaction 1 is that there is a barrier associated with formation of  $V^+(a^5D)$  and that the threshold observed for reaction 1,  $\sim 1.2$  eV, is a

measure of this barrier height. Such a barrier could be associated with the four-centered transition state that we have proposed<sup>6</sup> as the likely path for forming a  $D-V^+-OD$  intermediate from  $VO^+ + D_2$ , or with the tight transition state corresponding to reductive elimination of  $D_2O$  from this same intermediate. The present study of the reverse of reaction 1 is a simple way to test these two interpretations and to understand this system in more detail.

## Experimental Section

**General.** Complete descriptions of the apparatus and experimental procedures are given elsewhere.<sup>7</sup>  $V^+$  ions are produced as described below. The ions are extracted from the source, accelerated, and focused into a magnetic sector momentum analyzer for mass analysis. Mass-selected ions are slowed to a desired kinetic energy and focused into an octopole ion guide that radially traps the ions. The octopole passes through a static gas cell containing the neutral reactant at pressures sufficiently low ( $< 0.07$  mTorr) that multiple ion-molecule collisions are improbable. Upon exiting the gas cell, product and unreacted beam ions drift to the end of the octopole where they are directed into a quadrupole mass filter for mass analysis and then detected. Ion intensities are converted to absolute cross sections as described previously.<sup>7</sup> Uncertainties in cross sections are estimated to be  $\pm 20\%$ .

Laboratory ion energies relate to center-of-mass (CM) frame energies by  $E_{CM} = E_{lab} m / (M + m)$  where  $M$  and  $m$  are the ion and neutral reactant masses, respectively. The experimental cross sections are broadened by two effects: the thermal motion of the neutral gas, which has a width of  $\sim 0.46 E_{CM}^{1/2}$  for the present system,<sup>8</sup> and the distribution of ion energies (fwhm = 0.3–0.5 eV lab). The zero of the absolute energy scale and the ion energy distribution are measured by a retarding potential technique described elsewhere.<sup>7</sup> The uncertainty in the absolute energy scale is  $\pm 0.05$  eV lab (0.014 eV CM).

**Ion Sources.** The  $V^+$  ions used in these experiments were produced in flow tube (FT), surface ionization (SI), and electron impact (EI) sources. The FT source utilizes a direct current discharge source<sup>9</sup> comprising a vanadium cathode held at 1.5–3 kV over which a flow of approximately 90% He and 10% Ar passes at a typical pressure of  $\sim 0.5$  Torr.  $Ar^+$  ions created in the discharge are accelerated toward the vanadium cathode, sputtering off ionic metal atoms. The ions then undergo  $\sim 10^5$  collisions with He and  $\sim 10^4$  collisions with Ar in the meter-long flow tube before they enter the guided-ion-beam apparatus. Because collisions with He do not effectively quench most excited electronic states of transition metal ions,<sup>10</sup> methane gas is

<sup>†</sup> Present address: Department of Chemistry, Northwestern University, 2145 Sheridan, Evanston, IL 60208.

<sup>‡</sup> Present address: Institute for Chemical Education, Department of Chemistry, University of Wisconsin, 1101 University Avenue, Madison, WI 53706.

\* Abstract published in *Advance ACS Abstracts*, July 1, 1994.

TABLE 1: V<sup>+</sup> State Populations for EI and SI Beams

state	config	energy, <sup>a</sup> eV	% population		
			2000 K SI <sup>b</sup>	2200 K SI <sup>b</sup>	30 eV EI <sup>c</sup>
a <sup>5</sup> D	3d <sup>4</sup>	0.026	83.25	80.55	40
a <sup>5</sup> F	4s3d <sup>3</sup>	0.36	16.58	19.14	18
a <sup>3</sup> F	4s3d <sup>3</sup>	1.10	0.135	0.23	7
a <sup>3</sup> P	3d <sup>4</sup>	1.45	0.008	0.016	} 10
a <sup>3</sup> H	3d <sup>4</sup>	1.57	0.014	0.031	
b <sup>3</sup> F	3d <sup>4</sup>	1.68	0.005	0.011	
a <sup>5</sup> P	4s3d <sup>3</sup>	1.69	0.003	0.007	} 25
others	4s3d <sup>3</sup>	≥2.37	<0.01	<0.01	

<sup>a</sup> Energies are a statistical average over the J levels. <sup>b</sup> Surface ionization. Population calculated by assuming a Maxwell-Boltzmann distribution. <sup>c</sup> Electron impact ionization of VOCl<sub>3</sub>. Population estimates from refs 3, 16, and 10. See text.

introduced ~25 cm downstream from the discharge at pressures of 1–5 mTorr such that the ions are calculated to undergo 10<sup>2</sup>–10<sup>3</sup> collisions with methane in the flow tube. Vanadium ions in their a<sup>3</sup>F and higher lying states are known to react efficiently at thermal energies with methane,<sup>3</sup> thus eliminating these states from the ion beam. This was verified by examining the reaction of these V<sup>+</sup> ions with methane in the collision cell and comparing to our previous state-specific results,<sup>3</sup> as discussed previously.<sup>11</sup> Analysis of these results also shows no evidence for the presence of the a<sup>5</sup>F state of V<sup>+</sup>. Thus, we believe that the ions produced in the FT source are exclusively in their a<sup>5</sup>D ground state, and we assume the populations of the spin-orbit levels have a Maxwell-Boltzmann distribution at 300 K.

In the SI source, gaseous VOCl<sub>3</sub> (Alfa 99.995%) is directed at a resistively heated rhenium filament where decomposition of VOCl<sub>3</sub> and ionization of the resultant vanadium atoms take place. The temperature of the filament (2000 and 2200 K) is calibrated by optical pyrometry measurements and has an absolute uncertainty of ±100 K. It is generally assumed that a Maxwell-Boltzmann distribution accurately describes the populations of the electronic states of the ions. The validity of this assumption has been discussed previously<sup>12</sup> and recently verified by van Koppen et al. for Co<sup>+</sup>.<sup>13</sup> Table 1 gives these populations for V<sup>+</sup> produced at the filament temperatures used in the present experiments.

In order to produce V<sup>+</sup> beams that contain large fractions of excited state ions, we also used an EI source. In this source, 30 eV electrons ionize and dissociate VOCl<sub>3</sub> (Alfa 99.995%) vapor to form V<sup>+</sup>. Because the appearance energy of V<sup>+</sup> from VOCl<sub>3</sub> is 26.8 ± 0.4 eV,<sup>14</sup> it is possible to form significant percentages of excited state ions at an electron energy of 30 eV. The populations of the excited states of V<sup>+</sup> formed under these conditions have been studied in our laboratory<sup>3,15,16</sup> and also by Kemper and Bowers.<sup>10</sup> Results from both laboratories provide complementary information and yield the results listed in Table 1 for an electron energy of 30 eV. These populations are consistent with those given by Kemper and Bowers, although they assign 25% of the V<sup>+</sup> beam to states with 4s3d<sup>3</sup> configurations lying above 2.4 eV of excitation energy. In all of the systems that we have studied previously<sup>2,3,15</sup> and in the present work, no evidence of such high-lying states is observed for ions produced at 30 eV electron energies. This result can be interpreted to indicate that the population of states with excitation energies above 2.4 eV in the 30 eV EI V<sup>+</sup> beam is smaller than the 25% figure of Kemper and Bowers, or that these states are present but unreactive, or both. The answer to this dichotomy is to make the same population assignments as Kemper and Bowers with the single modification that part of the 25% high-energy population is attributed to the a<sup>5</sup>P state, 1.69 eV above the ground state. This assignment is consistent with Kemper and Bowers results because the a<sup>5</sup>P state has a 4s3d<sup>3</sup> electron configuration and consistent with our results because this state is likely to be unreactive because of its high spin and 4s orbital occupation.<sup>17,18</sup>

TABLE 2: Bond Energies at 0 K<sup>a</sup>

bond	D, eV
D—D	4.556 <sup>a</sup>
O—D	4.454(0.003) <sup>a</sup>
DO—D	5.212(0.003) <sup>a</sup>
V <sup>+</sup> —D	2.09(0.06) <sup>b</sup>
V <sup>+</sup> —O	5.99(0.10) <sup>c</sup>
V <sup>+</sup> —OD	4.41(0.19), <sup>d</sup> 4.50(0.15), <sup>e</sup> 4.64(0.13) <sup>f</sup>
V <sup>+</sup> —OD <sub>2</sub>	1.52(0.05), <sup>g</sup> 1.57(0.13), <sup>h</sup> 1.52(0.17) <sup>h</sup>

<sup>a</sup> Gurvich, L. V.; et al. *Thermodynamic Properties of Individual Substances*; Hemisphere: New York, 1989, Vol. 1, Part 2. <sup>b</sup> Reference 15. <sup>c</sup> Clemmer, D. E.; Elkind, J. L.; Aristov, N.; Armentrout, P. B. *J. Chem. Phys.* **1991**, *95*, 3387. <sup>d</sup> This work. <sup>e</sup> Reference 6. <sup>f</sup> Magera, T. F.; David, D. E.; Michl, J. *J. Am. Chem. Soc.* **1989**, *111*, 4100. 298 K values. <sup>g</sup> Reference 28. <sup>h</sup> Reference 5. 298 K value.

**Neutral Gas.** D<sub>2</sub>O was obtained from Cambridge in 99.9% purity. We found that it was critical to purge the D<sub>2</sub>O with dry N<sub>2</sub> gas before use in order to remove any oxygen that was dissolved in the D<sub>2</sub>O liquid. Results for the reaction of V<sup>+</sup> with D<sub>2</sub>O that had not been purged before use were drastically different than the data obtained after the liquid had been purged. The main difference was the presence of a large exothermic feature in the VO<sup>+</sup> data channel resulting from reaction of V<sup>+</sup> with O<sub>2</sub>. In addition, VOD<sup>+</sup> was also formed exothermically by a path that could not be ascertained unequivocally but may involve reaction of D<sub>2</sub>O with excited VO<sup>+</sup> ions formed in the reaction of V<sup>+</sup> with O<sub>2</sub>.

**Thermochemical Analyses.** Theory<sup>19</sup> and experiment<sup>20</sup> indicate that cross sections for endothermic reactions can be modeled by eq 2, which involves an explicit sum of the contributions of

$$\sigma(E) = \sigma_0 \sum_i g_i (E + E_i + E_{\text{int}} - E_0)^n / E \quad (2)$$

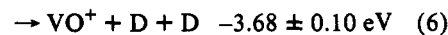
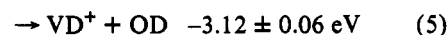
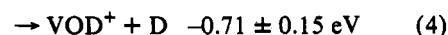
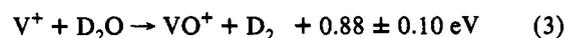
individual electronic states of the V<sup>+</sup> reactant, denoted by *i*, having energies *E<sub>i</sub>* and populations *g<sub>i</sub>*. Here,  $\sigma_0$  is a scaling factor, *E* is the relative kinetic energy, *E<sub>int</sub>* is the internal energy of the D<sub>2</sub>O reactant at 300 K (0.039 eV), *n* is an adjustable parameter, and *E<sub>0</sub>* is the threshold for reaction of the lowest electronic level of the ion, V<sup>+</sup>(a<sup>5</sup>D<sub>0</sub>). When data obtained for V<sup>+</sup> generated by EI are analyzed, the thresholds reported are given as *E<sub>T</sub>* = *E<sub>0</sub>* - *E<sub>i</sub>*. Error limits for *E<sub>0</sub>* are calculated from the range of threshold values for different data sets, variations in the parameter *n*, and the absolute error in the energy scale.

Some data channels also require a modified form of eq 2 that accounts for a decline in the product ion cross section at higher energies. This model has been described in detail previously.<sup>21</sup>

Because of the attractive interaction between the ion and the polarizable neutral molecule, there are often no activation barriers in excess of the endothermicity of ion-molecule reactions.<sup>20</sup> Thus, the reaction thresholds measured here are anticipated to equal the enthalpy difference between reactants and products. In the present system, the thermochemistry of the reactants and products are known (Table 2) such that this assumption can be directly tested.

## Results

Vanadium ions can react with D<sub>2</sub>O to form three ionic products, VO<sup>+</sup>, VOD<sup>+</sup>, and VD<sup>+</sup>, in reactions 3–6.



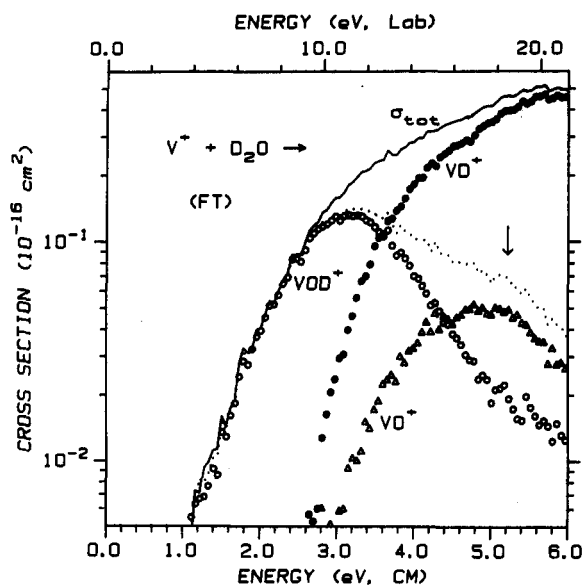


**Figure 1.** Variation of product cross sections for reaction of  $D_2O$  with  $V^+$  produced in the flow tube (FT) source as a function of translational energy in the center-of-mass frame (lower scale) and laboratory frame (upper scale). The solid line is the sum of the cross sections for all products. The dotted line is the sum of  $\sigma(VO^+)$  and  $\sigma(VOD^+)$ . The arrow shows the bond energy of  $D_0(DO-D)$  at 5.21 eV.

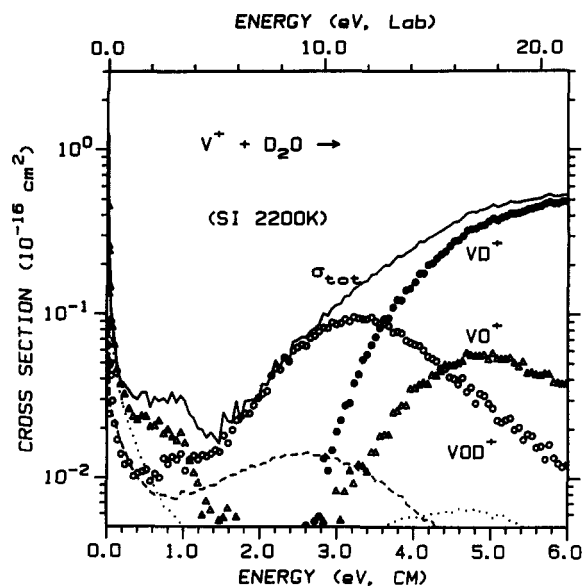


**Figure 2.** Variation of product cross sections for reaction of  $D_2O$  with  $V^+$  produced by surface ionization (SI) as a function of translational energy in the center-of-mass frame (lower scale) and laboratory frame (upper scale). The solid line is the sum of the cross sections for all products. The dashed and dotted lines show the cross sections for  $VOD^+$  and  $VO^+$ , respectively, taken from Figure 3 and scaled by a factor of 0.035.

**TABLE 3: Summary of Parameters of Eq 2<sup>a</sup>**

product	source <sup>b</sup>	$E_T$ , eV <sup>c</sup>	$\sigma_0$	$n$
$VO^+$	FT( $a^5D$ )	3.55(0.16)	0.2(0.1)	0.7(0.2)
$VOD^+$	FT( $a^5D$ )	0.79(0.19)	0.03(0.02)	3.1(0.3)
	EI <sup>d</sup>	0.4(0.3)	0.10(0.03)	1.6(0.3)
$VD^+$	FT( $a^5D$ )	3.07(0.10)	0.7(0.2)	1.3(0.1)
	EI	2.14(0.12)	0.9(0.2)	1.6(0.3)

<sup>a</sup> Uncertainties in parentheses. <sup>b</sup> This refers to the source used to produce the  $V^+$  reactant; FT, flow tube; EI, electron impact. <sup>c</sup>  $E_T = E_0 - E_i$  in eq 2. <sup>d</sup> Analysis performed after the exothermic feature is subtracted, as described in the text.

The thermodynamics indicated are calculated from the bond energies listed in Table 2 and correspond to reaction of ground state  $V^+(a^5D)$  to form ground state products at 0 K.  $D_2O$  rather than  $H_2O$  is used in order to enhance mass resolution yet enable operation of the guided-ion-beam instrument under conditions that optimize efficient product collection.

$V^+(a^5D) + D_2O$ . Results for reaction of  $D_2O$  with  $V^+(a^5D)$  produced in the flow tube source are shown in Figure 1. All processes observed are endothermic, and there is clearly no evidence for the exothermic reaction 3, the reverse of reaction 1. Instead, the  $VO^+$  product that is observed does not begin until about 3 eV. Analysis of this cross section with eq 2 gives a threshold of  $3.55 \pm 0.16$  eV (Table 3) which confirms that the  $VO^+$  observed can be explained exclusively by reaction 6. There is a small tail at low energies on this cross section that barely exceeds the experimental sensitivity of  $\sim 10^{-19}$  cm<sup>2</sup>, but this has an energy dependence that is consistent with overlap from the much more intense  $VOD^+$  product. We conclude that reaction 3 does not occur within our experimental sensitivity.

The lowest energy reaction that is observed is formation of  $VOD^+$  in reaction 4. The cross section for this reaction rises slowly from an apparent onset below 1.0 eV, close to the calculated thermodynamic threshold. Analysis of the cross section with eq 2 and the parameters listed in Table 3 yields a threshold of  $0.79 \pm 0.19$  eV in good agreement with the literature thermochemistry. At kinetic energies above about 3 eV, the cross section for  $VOD^+$  declines. This product can dissociate to form either  $VO^+ + D$ , from the overall reaction 6, or  $V^+ + OD$ , by a channel that cannot begin until 5.21 eV =  $D_0(DO-D)$  (Table 2). Thus, only the former dissociation channel can explain the observed behavior,

but the sum of the  $VOD^+$  and  $VO^+$  cross sections still peaks near 3 eV (Figure 1). This indicates that competition with formation of  $VD^+$  (reaction 5) must also influence the probability of  $VOD^+$  formation. Competition between formation of  $VD^+$  and  $VOD^+$  is consistent with the smooth appearance of the total cross section (Figure 1). The  $VD^+$  channel, which dominates the products at elevated energies, has a threshold measured to be  $3.07 \pm 0.10$  eV (Table 3) in good agreement with the calculated thermochemistry. Thus, there are no barriers in excess of the reaction endothermicity for any of the three reactions observed here, processes 4–6.

The qualitative features of these cross sections are similar to those previously reported for the interaction of  $V^+$  with ammonia and methane.<sup>2,3</sup> Competition between formation of  $VH^+$  and  $VNH_2^+$  or  $VCH_3^+$  (the isoelectronic analogues of  $VOD^+$ ) is also observed in the ammonia and methane systems, respectively. Furthermore, formation of  $VH^+$  (or  $VD^+$  in the present results) dominates in all three systems at high energies. The major difference between the reaction of  $V^+(a^5D)$  with water when compared to its reaction with ammonia and methane is that the dehydrogenation reactions to form  $VNH^+$  and  $VCH_2^+$  are observed while the analogous dehydrogenation reaction to form  $VO^+$ , reaction 3, is not. This difference is particularly notable because dehydrogenation of methane is endothermic, while dehydrogenation of ammonia and water are exothermic reactions. Another difference is that fewer products are observed in the water system because  $D_2O$  contains only three atoms. Thus, there is no product analogous to formation of  $VN^+$  and  $VCH^+$  observed in the ammonia and methane systems, respectively.

$V^+(SI) + D_2O$ . Results for reaction of  $D_2O$  with  $V^+$  produced in the surface ionization (SI) source at a filament temperature of 2200 K are shown in Figure 2. Above  $\sim 1.5$  eV of kinetic energy, the  $VD^+$ ,  $VO^+$ , and  $VOD^+$  cross sections are the same (within experimental error) as those for  $V^+(a^5D)$  shown in Figure 1. This indicates that the observed reactivity is dominated by the  $a^5D$  state. The  $a^5F$  state, which comprises 19% of the SI beam (Table 1), must be fairly unreactive; otherwise we should observe shifts in the thresholds for the  $VD^+$  and  $VO^+$  cross sections.

The differences between the  $a^5D$  and SI data appear below 1.5 eV kinetic energy. Here, both the  $VO^+$  and  $VOD^+$  cross sections increase with decreasing energy to as low an energy as we can measure. This behavior indicates that these products are formed

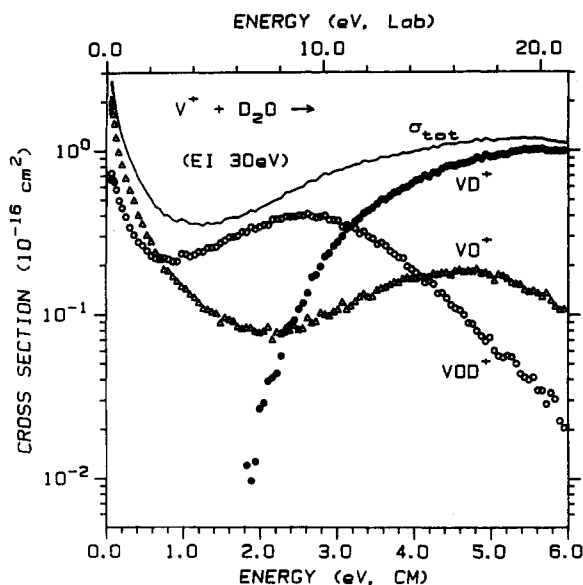


**Figure 3.** Variation of product cross sections for reaction of D<sub>2</sub>O with V<sup>+</sup> produced by electron impact ionization (EI) of VOCl<sub>3</sub> at 30 eV as a function of translational energy in the center-of-mass frame (lower scale) and laboratory frame (upper scale). The solid line is the sum of the cross sections for all products.

in barrierless exothermic reactions. Exothermic formation of VOD<sup>+</sup> must be due to electronic states of V<sup>+</sup> having excitation energies exceeding 0.7 eV, which comprise only 0.3% of the SI beam (Table 1). Exothermic formation of VO<sup>+</sup> must correspond to dehydrogenation of D<sub>2</sub>O, reaction 3, because the population of excited states having excitation energies exceeding 3.68 eV, the endothermicity of reaction 6, is much too small to account for the magnitude of the VO<sup>+</sup> cross section observed.

**V<sup>+</sup>(EI) + D<sub>2</sub>O.** Results for reaction of D<sub>2</sub>O with V<sup>+</sup> produced in the electron impact (EI) source at an electron energy of 30 eV are shown in Figure 3. Compared with the data for V<sup>+</sup>(a<sup>5</sup>D) (Figure 1), the cross sections for all products are larger and shifted to lower energies. The endothermic features in the EI cross sections all begin about 1 eV lower than the apparent thresholds for the V<sup>+</sup>(a<sup>5</sup>D) cross sections. This suggests that the triplet states with excitation energies near 1 eV (Table 1) are the dominant excited states present in the EI beam. At low energies, the EI data exhibit strong exothermic reactivity in the VO<sup>+</sup> and VOD<sup>+</sup> product channels. This is consistent with the much larger population of states having excitation energies exceeding 0.70 eV, as indicated in Table 1. Exothermic formation of VO<sup>+</sup> must correspond to dehydrogenation of D<sub>2</sub>O, reaction 3, because there is no evidence in the VD<sup>+</sup> channel or in our previous studies<sup>2,3,15</sup> that V<sup>+</sup> ion beams produced by EI at 30 eV include excited states having excitation energies exceeding 3.68 eV, the endothermicity of reaction 6.

A more quantitative assessment of the dominant excited states present in the EI beam can be made in two ways: from an analysis of the cross section for VD<sup>+</sup> and from a comparison of the SI and EI cross section magnitudes. Analysis of the VD<sup>+</sup>(EI) cross section with eq 2 yields the optimum parameters given in Table 3. The threshold of  $2.14 \pm 0.12$  eV is  $0.98 \pm 0.13$  eV lower than the value calculated for reaction of V<sup>+</sup>(a<sup>5</sup>D). This is evidence that the V<sup>+</sup>(a<sup>3</sup>F) state ( $E_i = 1.10$  eV) must be responsible for a large portion of the EI cross section, although contributions to the observed reactivity from higher-lying excited states ( $E_i \geq 1.45$  eV, Table 1) cannot be ruled out. Similar observations have been made in our previous studies of the reactions of V<sup>+</sup> with methane and ammonia.<sup>2,3</sup>

A comparison of the SI cross sections for VO<sup>+</sup> and VOD<sup>+</sup> with those from the EI data shows that the exothermic features in the SI data have the same energy dependence but are smaller by a

factor of  $0.035 \pm 0.005$ . This comparison is shown in Figure 2. On the basis of the state populations in Table 1, the SI beam contains 0.033 (= 0.23/7) times less a<sup>3</sup>F state than the EI beam. The ratio of populations of the a<sup>3</sup>P, a<sup>3</sup>H, and b<sup>3</sup>F states is 0.006 (= 0.058/10) and of higher lying states is much less. If all these excited states were equally reactive, then the SI/EI cross section ratio would be 0.017 (= 0.29/17), much less than the experimental ratio. SI data taken at a filament temperature of 2000 K were also obtained, and here the exothermic features are smaller than the EI data by a factor of  $0.023 \pm 0.004$ , again consistent with the calculated relative population of the a<sup>3</sup>F state, 0.019 (= 0.135/7), but not with that for the a<sup>3</sup>P, a<sup>3</sup>H, and b<sup>3</sup>F states, 0.003 (= 0.027/10), or the sum of these excited states, 0.010 (= 0.16/17). These comparisons strongly indicate that the a<sup>3</sup>F state dominates the exothermic reactivity observed in the EI data. If this is correct, the observed behavior indicates that either the population of the higher-lying states in the EI beam is lower than that listed in Table 1 or these states are relatively unreactive compared to the a<sup>3</sup>F state. The latter explanation is the only one consistent with our data and the results of Kemper and Bowers.<sup>10</sup>

The comparison of the SI and EI data in Figure 2 reveals an additional feature in the SI cross sections for VO<sup>+</sup> and VOD<sup>+</sup>. It can be seen that the low-energy exothermic portion of the SI and EI data below about 0.3 eV have nearly identical shapes but that the SI data are larger than the scaled EI data between 0.3 and 1.5 eV. These features cannot be attributed to the a<sup>3</sup>D and a<sup>3</sup>F states because their cross sections are already accounted for. Neither can they be due to the excited states with  $E_i > 1.1$  eV because the populations of these states increase in going from the SI to EI beams (Table 1), such that they should be much more prominent in the EI data, not less. By elimination, we attribute these cross section features to reaction of the a<sup>5</sup>F state of V<sup>+</sup>, whose population is nearly the same in the SI and EI beams (Table 1). This identification is consistent with the threshold for VOD<sup>+</sup> calculated for this state,  $0.34 \pm 0.15$  eV. Production of VO<sup>+</sup> + D<sub>2</sub> from the a<sup>5</sup>F state is calculated to be exothermic, behavior that could be consistent with our observations but that cannot be confirmed unequivocally because this cross section is obscured by the reactivity of the a<sup>3</sup>F excited state at the lowest kinetic energies.

**State-Specific Cross Sections.** Because the populations of V<sup>+</sup> states for a beam produced by EI at an electron energy at 30 eV are reasonably well established (Table 1), we can combine the EI and FT(a<sup>5</sup>D) results in order to estimate the cross sections associated with reaction of the excited triplet (a<sup>3</sup>F, a<sup>3</sup>P, a<sup>3</sup>H, and b<sup>3</sup>F) states of V<sup>+</sup>. Although the a<sup>3</sup>F state appears to dominate this reactivity, we refer to these states collectively as the <sup>3</sup>X state because the individual contributions that these states make to the 30 eV EI data cannot be distinguished unambiguously. To derive this cross section, we scale the a<sup>5</sup>D cross section by a factor of 40% (Table 2), subtract this from the EI data, and scale the remaining cross sections (due to 17% population of triplet states in the EI beam) to 100% to obtain  $\sigma(^3X)$ . This analysis ignores the contributions of the a<sup>5</sup>F first excited state, but these are small and have no noticeable effect on the <sup>3</sup>X cross sections. The end results are shown in Figure 4. They have energy dependences very similar to the EI data in Figure 3 but absolute magnitudes that are ~6 times larger. The absolute uncertainties in these cross sections are large because of the uncertainty in the relative reactivity of the different triplet states as a function of energy. The magnitudes obtained are reasonable, however, based on a comparison with the collision cross section.<sup>22</sup> We find that the total <sup>3</sup>X cross section is about 20% of the collision cross section at 0.1 eV.

A comparison of the reaction efficiencies for the a<sup>5</sup>D and <sup>3</sup>X states of V<sup>+</sup> shows that the latter have cross sections that are about 10–20 times larger at higher energies. For the dehydrogenation reaction,  $\sigma(\text{VO}^+, ^3X)$  has a magnitude of  $9 \text{ \AA}^2$  at ~0.1

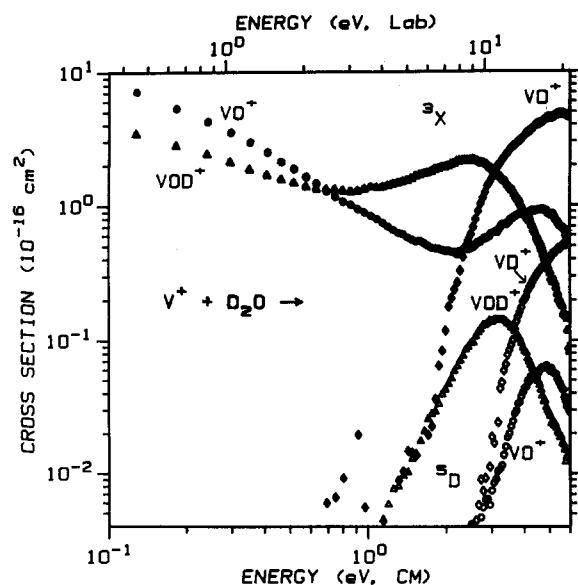


**Figure 4.** State-specific cross sections for the reaction of  $D_2O$  with  $V^+$  as a function of translational energy in the laboratory (upper axis) and center-of-mass frame (lower axis). Solid and open symbols show results for  $V^+(^3X)$  and  $V^+(^3D)$ , respectively, derived as discussed in the text.

eV while  $\sigma(VO^+, a^3D) \leq 0.003 \text{ \AA}^2$  (the sensitivity of our experiment). This comparison suggests that the triplet states are more efficient at dehydrogenation of  $D_2O$  by a factor of  $\geq 3000$ . Also for this reaction, the magnitude of the feature attributed to the  $a^3F$  state is about 20 times smaller than the  $^3X$  cross section from 0.5 to 1.0 eV.

One interesting aspect of the  $^3X$  cross sections is that both the  $VO^+$  and  $VOD^+$  cross sections exhibit behavior consistent with exothermic reactions at low kinetic energies but then increase at higher energies. The endothermic feature in the  $VO^+$  cross section is attributable to reaction 6 because it begins at an energy consistent with this process for excited electronic states,  $2.58 \pm 0.10$  eV for  $V^+(a^3F)$ . The endothermic feature in the  $VOD^+$  cross section is less straightforward to explain. An approximate analysis of this endothermic feature is performed by subtracting a power law fit to the exothermic portion of the  $^3X$  cross section from these data. Analysis of the remaining cross section with eq 2 gives a threshold of  $E_T = 0.40 \pm 0.30$  eV. An interesting possibility is that this endothermic portion of the  $^3X$  cross section is due to reaction of the "missing"  $a^3P$ ,  $a^3H$ , and  $b^3F$  states, which are less reactive because they must surmount an activation barrier of  $0.4 \pm 0.3$  eV. Another possibility is that there are two pathways for reaction of  $V^+(a^3F)$  to form  $VOD^+ + D$ . These explanations are discussed further below.

## Discussion

**Reaction Mechanism.** The reaction mechanisms for the interaction of  $V^+$  with ammonia and methane are similar to one another and have been described previously.<sup>2,3</sup> In this section, ideas from the ammonia and methane systems are extended to describe the interaction of  $V^+$  with water. In addition to explaining the product formation and the state-specific reactivity in the present system, this mechanism must also be consistent with our previously reported results for reaction 1.<sup>6</sup>

An obvious mechanism that can explain the observed competition between the  $VD^+$  and  $VOD^+$  products is oxidative addition of the O—D bond at the metal center to form  $D—V^+—OD$ , intermediate I. Bond additivity estimates show that formation of I from ground state reactants is exothermic by  $\sim 1.3$  eV. (More sophisticated estimates that include consideration of promotion energy effects yield a very similar result, because the promotion energy for two covalent bonds to  $V^+$  is approximately twice that for one covalent bond.<sup>23</sup>) At elevated energies, I decomposes by

V—D bond cleavage to form  $VOD^+ + D$  or by V—O bond cleavage to form  $VD^+ + OD$ .  $VOD^+$  is thermodynamically favored (Table 2), but  $VD^+$  formation dominates at high energies because of angular momentum constraints that have been described previously.<sup>2,3</sup> At high energies,  $VO^+$  can be formed by decomposition of  $VOD^+$  in reaction 6.

We envision three possible mechanisms for the dehydrogenation process 3: 1,1- $D_2$  loss from intermediate II or III; 1,2- $D_2$  loss from I via the four-center transition state IV. Intermediate II



is the ion-dipole complex formed in the initial interaction of  $V^+$  with water, and III is formed by an  $\alpha$ -D transfer from I. In the reactions of  $V^+$  with ammonia and methane, we concluded that the dehydrogenation reactions probably proceed by an intermediate analogous to I and the transition state IV. A similar conclusion was drawn in our study of reaction 1,<sup>6</sup> although excited triplet states of intermediate II (which is a ground state quintet)<sup>24</sup> could also be used to explain the observations made there. Intermediate III is ruled out on the basis of its relative thermodynamic instability<sup>25</sup> and the observation that it should have a singlet spin ground state if the bonds shown are covalent.<sup>6</sup> On the basis of these comparisons, we conclude that the dehydrogenation reaction occurs primarily via I and IV, a pathway consistent with the competitive behavior observed for the  $VOD^+$  and  $VD^+$  products.

**Electronic State Dependence.** In order to understand the effects of electronic states upon product formation, molecular orbital ideas can be employed. These arguments have been used successfully to elucidate reactivity and mechanisms in the reactions of  $V^+$  and other atomic metal ions with  $H_2$ ,  $CH_4$ , and  $NH_3$ .<sup>1-3,15</sup> These ideas show that if the metal 4s orbital (and to a lesser extent the 3d $\sigma$ ) is occupied, the interaction of the metal ion with water will be repulsive at short range because the 4s (3d $\sigma$ ) orbital correlates to an antibonding orbital of the intermediate. Oxidative addition of O—D to a metal center can be achieved by donation of electrons in  $\sigma$  bonding orbitals into empty 4s and 3d $\sigma$  orbitals on the metal and back-donation of metal 3d $\pi$  electrons into  $\sigma^*$  antibonding orbitals. This increases the electron density between the metal and molecular fragments and also lengthens the O—D bond. If oxidative addition forms I, which contains covalent V—D and V—O single bonds, then two of the valence electrons on  $V^+$  are involved in bonding, the other two are in nonbonding orbitals, and the ground state of I should have triplet spin. Finally, we note that the ground state of the dehydrogenation products also has triplet spin,  $VO^+(^3\Sigma^-) + D_2(^1\Sigma_g^+)$ . Excited states of  $VO^+$  include a  $^3\Delta$  that is 1.17 eV higher in energy and quintet states that are 3.3–4.2 eV higher in energy.<sup>26</sup> The ground states of the other two product channels are  $VD^+(^4\Delta)^{27} + OD(^2\Pi)$  and  $D(^2S) + VOD^+$  (presumed to have a quartet spin ground state as noted in previous work).<sup>6</sup>

On the basis of these ideas, the potential energy surfaces shown in Figure 5 can be drawn. This diagram shows an initial interaction of  $V^+$  with  $D_2O$  that is attractive for all states because of the ion-dipole potential. The depth of the V— $OD_2$  well for the ground state is  $\sim 1.5$  eV<sup>28</sup> (Table 2). The first state having the correct spin and electron configuration to smoothly generate the ground state of I is  $V^+(a^3P, 3d^4)$ , but these surfaces undergo avoided crossings with the surfaces evolving from the  $a^3F(4s^1-3d^3)$  state. These surface interactions are equivalent to moving the 4s electron into one of the 3d orbitals in order to remove the repulsive interactions with  $D_2O$ . The high-spin  $V^+(a^5D, 3d^4)$  state correlates with an excited state of I and therefore must cross the low-spin triplet surfaces. The high-spin  $V^+(a^5F, 4s^1 3d^3)$  state has

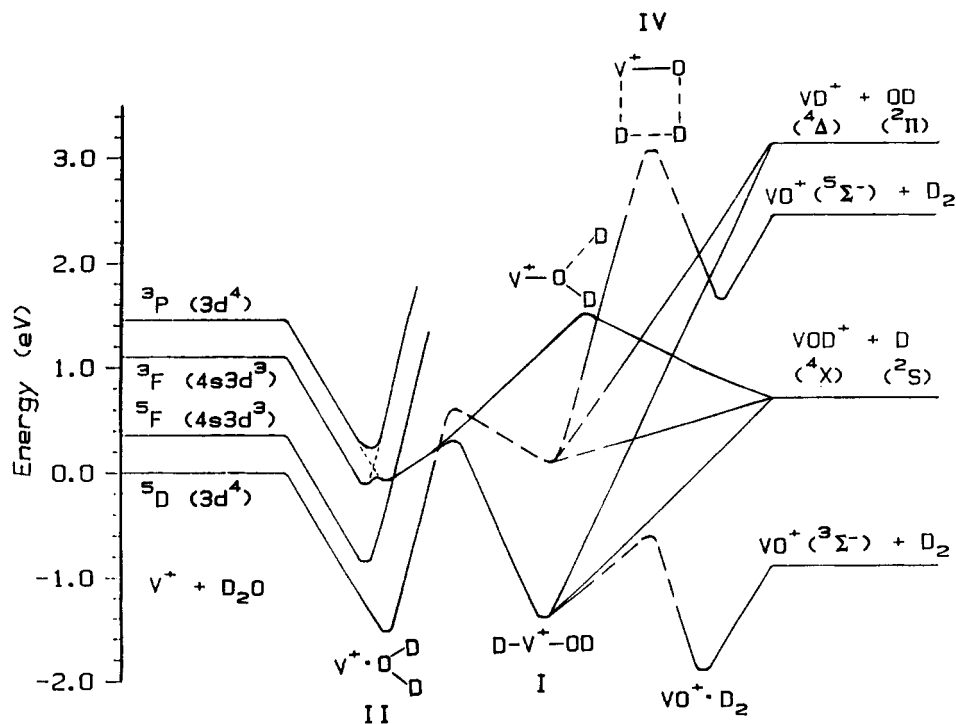


**Figure 5.** Semiquantitative potential energy surfaces for the reaction of the four lowest energy states of  $V^+$  with  $D_2O$  to form  $VD^+$ ,  $VO^+$ , and  $VOD^+$ . For simplicity, only two states of  $VO^+$  are shown. Short dashed lines indicate an avoided surface crossing. Long dashed lines indicate that no experimental information is available to allow a quantitative estimate of the energy.

both the wrong spin and wrong electron configuration to form the ground state of I and should be repulsive at short range.

Given these surfaces, we can now explain the observed reactivity of the various states of  $V^+$  with  $D_2O$ . Efficient formation of  $VO^+ + D_2$ ,  $VOD^+ + D$ , and  $VD^+ + OD$  from the triplet excited states is easily explained because these reactions are all spin-allowed and can proceed via the ground state of I. The observation that exothermic formation of  $VOD^+ + D$  and  $VO^+ + D_2$  in the SI and EI data is largely due to the  $a^3F$  state, even though the higher-lying  $a^3P$ ,  $a^3H$ , and  $b^3F$  states are present, may be a result of the avoided surface interaction between these states as shown in Figure 5.

As noted above, there is apparently a second pathway for formation of  $VOD^+$  from the triplet state reactants that involves a reaction barrier measured to be  $\sim 0.4 \pm 0.3$  eV above the reactant energy. This could be due to the "missing"  $a^3P$ ,  $a^3H$ , and  $b^3F$  states, but this bimodal type of reactivity has been observed before for the reactions of metal ions with methanol and methyl chloride.<sup>29,30,31</sup> In these cases, other states cannot be used to explain the bimodal behavior, and we have attributed it to an insertion mechanism at low energies and a more direct mechanism at higher energies. In the present case, the direct mechanism corresponds to cleavage of an O—D bond in intermediate II,  $V^+—OD_2$ . A qualitative explanation for the origin of a barrier for this process can be seen by considering the molecular orbitals involved in the reverse process, approach of a deuterium atom to  $VOD^+$ . The  $VOD^+$  molecule, as previously discussed,<sup>6</sup> is likely to have a quartet ground state with the unpaired electrons located primarily on the vanadium atom in nonbonding orbitals. Thus, addition of a deuterium atom to the vanadium end of  $VOD^+$  (which forms I) should lead to an attractive covalent interaction (Figure 5). Addition of a deuterium atom to the oxygen atom in  $VOD^+$  (which forms II), however, should be more repulsive because all of the orbitals on the oxygen atom are filled. This repulsive interaction could lead to the barrier observed experimentally here and is shown in Figure 5.

The reactivity of the low-lying quintet states of  $V^+$  is more complex to explain. In order to dehydrogenate water in an exothermic reaction, ground state  $V^+(a^5D)$  must cross to the

low-spin triplet surfaces, a surface coupling that requires spin-orbit interactions. This coupling is apparently very weak because no  $VO^+ + D_2$  is observed for this state and the reverse of reaction 1 is not observed. Production of  $VOD^+ + D$  and  $VD^+ + OD$  at their thermodynamic thresholds must therefore proceed by formation of an excited high-spin state of I in spin-allowed processes. Spin-allowed dehydrogenation of water to form quintet states of  $VO^+ + D_2$ , which must pass through a tight transition state, is too high in energy to compete effectively with the other two channels that can be formed by simple bond fission processes.

We now want to explain why  $V^+(a^5D)$  dehydrogenates methane and ammonia,<sup>2,3</sup> but not water, even though the methane reaction is endothermic while the water reaction is exothermic. A speculative explanation for this difference lies in the relative bond strengths:  $D_0(DO—D) = 5.21$  eV  $>$   $D_0(H_2N—H) = 4.70$  eV  $>$   $D_0(H_3C—H) = 4.48$  eV. This should influence the height of the barrier corresponding to insertion of  $V^+$  into these bonds (or equivalently, reductive elimination of the molecule from the intermediates analogous to I). This will influence the position of the crossing between the quintet and triplet surfaces (Figure 5). Indeed, if the energy of this surface crossing is above the energy of the ground state reactant asymptote (which is most likely for  $D_2O$  because of the relative energetics cited above), it seems likely that the efficiency of switching from the quintet to the triplet surfaces should be much less than if the surface crossing is below the asymptotic energy.

This hypothesis can also help explain the contrast between the inertness of the  $V^+(a^5D)$  state and the apparent observation that  $V^+(a^5F)$  does dehydrogenate water at low kinetic energies (albeit very inefficiently) and that the reverse reaction 1 appears to form this state. The only explanation that we can imagine is that this depends on the details of how the surfaces evolving from these two high-spin states interact with the low-spin states leading to the ground state of I. In particular, the difference in reactivity can be explained reasonably if the  $V^+(a^5F) + D_2O$  asymptote lies above the energy where its surface crosses that evolving from the excited triplet states.

Finally, we return to the question asked in the Introduction of whether the elevated threshold of  $\sim 1.2$  eV observed for reaction

1 is because of reaction barriers or preferential formation of excited states. We reject the possibility that this threshold corresponds to transition state IV. We believe that we have measured the energy of this transition state for the reactions of  $\text{FeO}^+$  and  $\text{CoO}^+$  with  $\text{D}_2$  and find them to lie 0.62 and 0.75 eV above the  $\text{MO}^+ + \text{D}_2$  asymptote.<sup>32,33</sup> It seems unlikely that this transition state would lie twice as high in energy in the vanadium system (where there are empty orbitals available to facilitate this interaction). The possibility that the 1.2 eV threshold corresponds to the transition state associated with D—OD bond activation (between intermediates I and II) is a reasonable one and helps explain the state-specific reactivity observed in the present study; however, the present work is also completely consistent with the idea that reaction 1 preferentially reacts to form  $\text{V}^+$  states in spin-conserving reactions. Both spin-conservation and a barrier to D—OD bond activation are needed to explain all the details of the present results, those for reaction 1, and the differences in the reactivities of  $\text{V}^+(\text{a}^5\text{D})$  with  $\text{D}_2\text{O}$ ,  $\text{NH}_3$ , and  $\text{CH}_4$ . The energy of this insertion barrier cannot be assigned unambiguously, given the information presently available.

**Acknowledgment.** This work is supported by the National Science Foundation, Grant No. CHE-9221241.

### References and Notes

- (1) Armentrout, P. B. In *Gas Phase Inorganic Chemistry*; Russell, D. H., Ed.; Plenum: New York, 1989; p 1. Armentrout, P. B.; Beauchamp, J. L. *Acc. Chem. Res.* **1989**, *22*, 315. Armentrout, P. B. In *Selective Hydrocarbon Activation: Principles and Progress*; Davies, J. A., Watson, P. L., Liebman, J. F., Greenberg, A., Eds.; VCH: New York, 1990; p 467.
- (2) Clemmer, D. E.; Sunderlin, L. S.; Armentrout, P. B. *J. Phys. Chem.* **1990**, *94*, 3008.
- (3) Aristov, N.; Armentrout, P. B. *J. Phys. Chem.* **1987**, *83*, 6178.
- (4) Bent, H. A. *J. Chem. Educ.* **1966**, *43*, 170.
- (5) Marinelli, P. J.; Squires, R. R. *J. Am. Chem. Soc.* **1989**, *111*, 4101.
- (6) Clemmer, D. E.; Aristov, N.; Armentrout, P. B. *J. Phys. Chem.* **1993**, *97*, 544.
- (7) Ervin, K. M.; Armentrout, P. B. *J. Chem. Phys.* **1985**, *83*, 166.
- (8) Chantry, P. J. *J. Chem. Phys.* **1971**, *55*, 2746.
- (9) Schultz, R. H.; Crellin, K. C.; Armentrout, P. B. *J. Am. Chem. Soc.* **1991**, *113*, 8590.
- (10) Kemper, P. R.; Bowers, M. T. *J. Phys. Chem.* **1991**, *95*, 5134.
- (11) Chen, Y.-M.; Clemmer, D. E.; Armentrout, P. B. *J. Chem. Phys.* **1993**, *98*, 4929.
- (12) Sunderlin, L. S.; Armentrout, P. B. *J. Phys. Chem.* **1988**, *92*, 1209.
- (13) van Koppen, P. A. M.; Kemper, P. R.; Bowers, M. T. *J. Am. Chem. Soc.* **1992**, *114*, 10941.
- (14) Flesch, G. D.; Svec, H. J. *Inorg. Chem.* **1975**, *14*, 1817.
- (15) Elkind, J. L.; Armentrout, P. B. *J. Phys. Chem.* **1985**, *89*, 5626.
- (16) Clemmer, D. E. Ph.D. Thesis, University of Utah, 1992.
- (17) Armentrout, P. B. *Annu. Rev. Phys. Chem.* **1990**, *41*, 313.
- (18) Armentrout, P. B. *Science* **1991**, *251*, 175.
- (19) Chesnavich, W. J.; Bowers, M. T. *J. Phys. Chem.* **1979**, *83*, 900.
- (20) Sunderlin, L. S.; Aristov, N.; Armentrout, P. B. *J. Am. Chem. Soc.* **1987**, *109*, 78. Armentrout, P. B. *Advances in Gas Phase Ion Chemistry*; JAI: Greenwich, 1992; Vol. 1, p 83.
- (21) Weber, M. E.; Elkind, J. L.; Armentrout, P. B. *J. Chem. Phys.* **1986**, *84*, 1521.
- (22) We use the simple Langevin-Gioumousis-Stevenson (LGS) form of the cross section,  $\sigma_{\text{LGS}} = \pi e(2\alpha/E)^{1/2}$ , where  $e$  is the unit of electric charge,  $\alpha$  is the polarizability of water, and  $E$  is the relative translational energy; Gioumousis, G.; Stevenson, D. P. *J. Chem. Phys.* **1958**, *29*, 294.
- (23) Armentrout, P. B.; Clemmer, D. E. In *Energetics of Organometallic Species*; Simoes, J. A. M., Ed.; Kluwer: Dordrecht, Netherlands, 1992; pp 321–356. Armentrout, P. B.; Kickel, B. L. In *Organometallic Ion Chemistry*; Freiser, B. S., Ed.; accepted for publication.
- (24) Rosi, M.; Bauschlicher, C. W. *J. Chem. Phys.* **1990**, *92*, 1876.
- (25) On the basis of bond additivity arguments and the assumption that the V—O bond is a double bond, we estimate that this species lies  $1.3 \pm 0.2$  eV above the energy of  $\text{V}^+ + \text{D}_2\text{O}$ .
- (26) Dyke, J. M.; Gravenor, B. W. J.; Hastings, M. P.; Morris, A. *J. Phys. Chem.* **1985**, *89*, 4613.
- (27) Schilling, J. B.; Goddard, W. A.; Beauchamp, J. L. *J. Am. Chem. Soc.* **1987**, *108*, 582; *J. Phys. Chem.* **1987**, *91*, 5616. Pettersson, L. G. M.; Bauschlicher, C. W.; Langhoff, S. R.; Partridge, H. *J. Chem. Phys.* **1987**, *87*, 481.
- (28) Dalleska, N. D.; Honma, K.; Sunderlin, L. S.; Armentrout, P. B. *J. Am. Chem. Soc.* **1994**, *116*, 3519.
- (29) Fisher, E. R.; Sunderlin, L. S.; Armentrout, P. B. *J. Phys. Chem.* **1989**, *93*, 7375. Fisher, E. R.; Schultz, R. H.; Armentrout, P. B. *J. Phys. Chem.* **1989**, *93*, 7382.
- (30) Clemmer, D. E.; Aristov, N.; Armentrout, P. B. Unpublished results.
- (31) Chen, Y.-M.; Clemmer, D. E.; Armentrout, P. B. Manuscript in preparation.
- (32) Clemmer, D. E.; Chen, Y.-M.; Khan, F.; Armentrout, P. B. *J. Phys. Chem.* in press.
- (33) Chen, Y.-M.; Clemmer, D. E.; Armentrout, P. B. *J. Am. Chem. Soc.* in press.